COMPARISON OF PRESTRESS LOSSES IN THE SR18/SR516 PRECAST, PRESTRESSED HIGH-PERFORMANCE CONCRETE BRIDGE

Paul J. Barr, PhD, Dept. of Civil Engr., New Mexico State University, Las Cruces, NM
John F. Stanton, PhD, PE, Dept. of Civil Engr., University of Washington, Seattle, WA
Marc O. Eberhard, PhD, Dept. of Civil Engr., University of Washington, Seattle, WA

ABSTRACT

Five precast, prestressed girders made with high-performance concrete (HPC) were instrumented using vibrating-wire strain gages. The girders were used in a new bridge built in the state of Washington, and their long-term behavior was monitored for three years from the time of casting. The HPC girders appear to be functioning well under service loads. The measured change in concrete strain at the centroid of the prestressing strands was used to evaluate the change in prestress. The total measured prestress loss was as large as 28% of the total jacking stress. This loss is larger than would be expected for a girder made with conventional-strength concrete. The observed values of prestress losses for the instrumented girders were compared with values calculated using the recommended PCI and AASHTO LRFD procedures. The total calculated prestress losses ranged from 6% lower to 22% higher than the average total observed prestress losses. However, this agreement was not a result of either method accurately predicting each of the individual prestress loss components. Instead, the total changes in prestress compared well, because some predictions were too low (e.g., elastic shortening) and others were too high (e.g., creep and shrinkage, relaxation and deck casting).

Keywords: High-Performance Concrete, Bridge Girders, Instrumentation, Strains, Prestress Losses, Elastic Shortening, Creep, Shrinkage

INTRODUCTION

The availability of high-strength concrete promises to increase the span range and decrease the costs of many precast, prestressed concrete girder bridges. For this type of construction, the compressive strength of the concrete at the time the prestressing force is transferred to the concrete is particularly important; this so-called release strength limits the maximum prestressing force that can be applied to a cross-section. An increase in the release strength makes it possible to increase the prestressing force, and consequently, to design longer spans and more-widely spaced girders (for a given section), or to use shallower sections (for a given girder span and spacing).

The increased design flexibility has important economic implications. The option of designing longer spans reduces the number of supports, which decreases construction costs and improves traffic safety, especially in congested locations. An increase in the maximum girder spacing reduces the number of girders, and thus, decreases fabrication, transportation and erection costs. If the depth of girders can be reduced, it is possible to increase underpass clearances or lower embankment heights.

Despite the apparent benefits of using high-strength concrete, some concerns have limited its widespread use in precast, prestressed girders. In particular, current methods for calculating prestress losses due to elastic shortening, creep and shrinkage were based on the observed behavior of conventional concrete, with compressive strengths usually below 41.4 MPa (6000 psi)[1,2]. These losses need to be predicted accurately, because incorrect estimates of prestress losses can lead to unacceptable service performance. The appropriateness of applying current design methods to high-strength concrete needs to be evaluated.

As part of a larger Federal Highway Administration (FHWA) program, which included various other lead states, the Washington State Department of Transportation (WSDOT) designed a new high-performance concrete (HPC) bridge to carry the eastbound lanes of State Route 18 (SR 18) over State Route 516 (SR 516). The girders were constructed of high-strength concrete, and the deck was constructed of high-durability concrete. The design, construction and monitoring of these girders provided the opportunity to assess the benefits and drawbacks of using high-strength concrete in prestressed concrete bridge girders. This paper documents the observed behavior of five girders and evaluates the accuracy of the AASHTO[1] and PCI[2] procedures for calculating prestress losses for these girders.

SR18/SR516 OVERCROSSING

Fig. 1 shows a plan view and elevation of the SR18/SR516 Overcrossing. The three-span bridge had two short, outside spans and a long, middle span. The lengths of these girders (accounting for the diaphragm thicknesses) were 23.3 m (76.7 ft) and 40.6 m (133 ft) for the short and long spans, respectively.

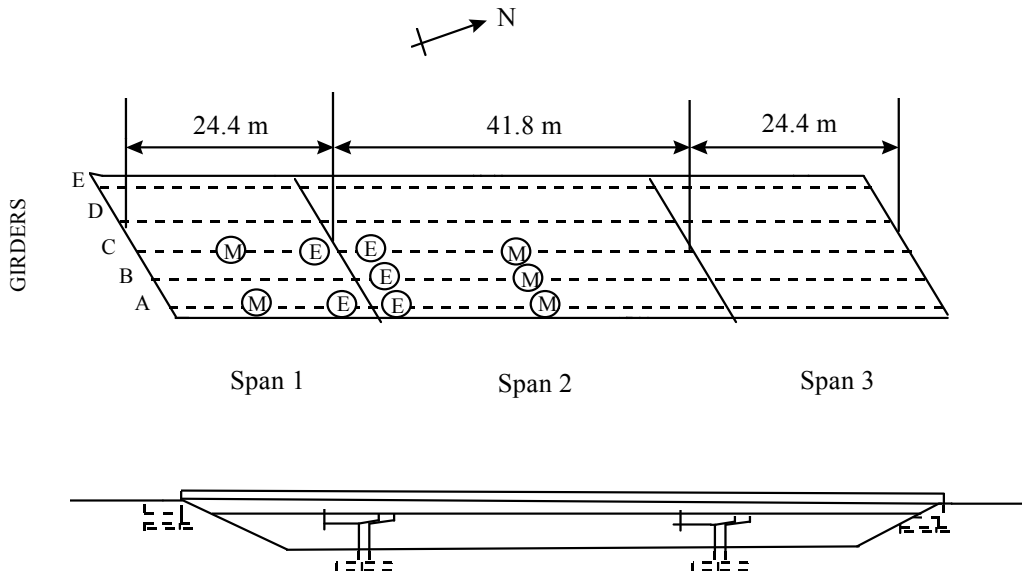

Fig. 1 Bridge Plan and Elevation

The Washington W74MG cross-section, shown in Fig. 2, was used for all of the girders. The girders were designed for HS 25 loading, for an allowable service tensile stress of zero, and for prestress losses calculated according to the Modified Rate of Creep Method[3]. The specified concrete compressive strengths were 68.9 MPa (10,000 psi) at 56 days and, more importantly, 51 MPa (7,400 psi) at the time of release of the prestressing strands. By increasing the release strength above its standard value, WSDOT designers were able to reduce the number of girder lines from seven to five, resulting in a nearly 30% decrease in the number of girders.

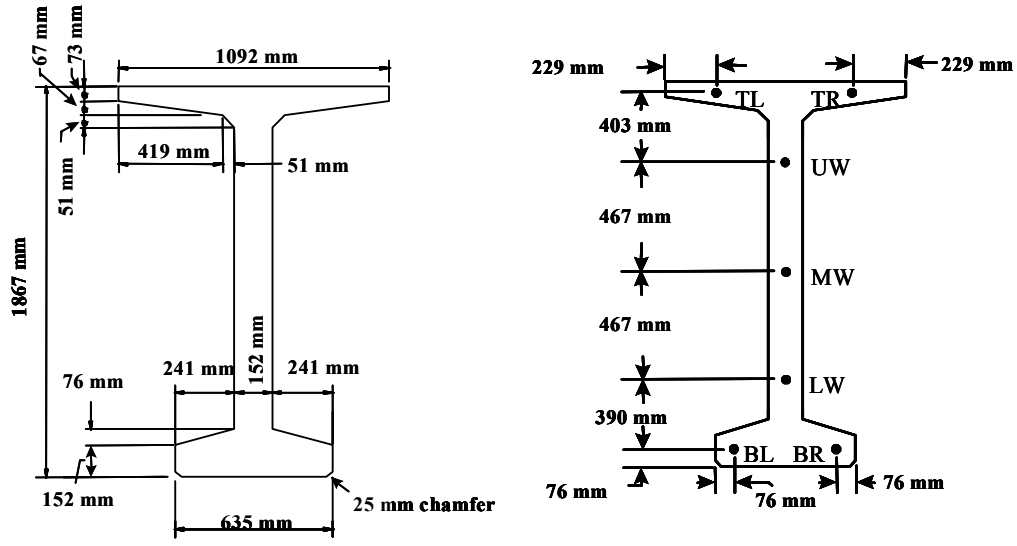

Fig. 2 Girder Cross-Section

To develop the required prestressing force while still satisfy strand spacing requirements, it was necessary to replace conventional 13-mm (0.5-in.) diameter strands with larger, 15-mm (0.6-in) strands. The long-span girders were prestressed with 14 harped strands in the web (harped at 0.4 times the girder length from each end) and 26 straight strands in the bottom flange. The short-span girders were prestressed with only 14 strands.

Table 1 summarizes the fabrication schedule for the five girders that were monitored. In this table, the individual girders are identified by span number (1 to 3) and girder line (A to E). For example, Girder 2C corresponds to the middle girder of the long span (Fig. 1). After casting, the girders were steam-cured under an insulated blanket until the match-cured concrete cylinders had attained the specified release strength. Because it took approximately 24 hours to attain the release strength, leaving no time for other fabrication operations within a one-day cycle, the fabricator operated on a two-day fabrication cycle. After destressing, the girders were stored in a fabrication yard until they were shipped to the bridge site. The girders were erected the night following the shipment date.

Table 1. Fabrication Schedule for Bridge Girders

Girder	Instrumentation Installation Date	Casting Date	Destressing Date	Time to Start of Destress (Hours)
2A	3/5/97	3/6/97	3/7/97	28.25
2B	3/9/97	3/10/97	3/11/97	25
2C	3/11/97	3/12/97	3/13/97	24
1A	4/1/97	4/2/97	4/3/97	24.25
1C	4/1/97	4/2/97	4/3/97	24.25

During the next five months after the girders were erected, the contractor worked on the bridge only intermittently. For example, the intermediate diaphragms were cast over a ten-day period in mid-July. The girders were finally made composite with a 190-mm (7.5 in.) thick deck on September 23, 1997, when the age of the monitored girders was approximately six months. The specified strength for the deck concrete was only 27.6 MPa (4000 psi), but it was also considered to be HPC, because the durability had been increased through the addition of fly-ash and by the requirement of a 14-day water cure.

MONITORING PROGRAM

Vibrating-wire strain gages (VSWG) with integral thermistors were embedded in three long-span girders (2A, 2B and 2C) and the two short-span girders (1A and 1B). These gages monitored concrete temperature and longitudinal strains at two sites in each girder: site M,

located near midspan; and site E, located 1.52 m (5 ft) from the girder end nearest Pier 2 (Fig. 1). Although not described here, the instrumentation program also included measurements of strand slip-back and girder camber[4].

Each site was instrumented as illustrated in Fig. 2. Two vibrating-wire strain gages (BL and BR) were embedded in the bottom flange of each girder at the centroid of the prestressing steel. Three gages (LW, MW and UW) were placed at the quarter points over the height of the girder web, and one gage (TG) was placed in the top flange of the girders. Later, two additional gages were also placed within the bridge deck.

The gages were monitored for approximately three years, beginning at the time of casting. During curing, the gages were monitored every fifteen minutes, but the reading interval decreased to one minute during destressing. After destressing, the gages were read at one-hour intervals for six months and subsequently, at six-hour intervals.

OBSERVED TEMPERATURES

The girder instrumentation provided nearly continuous temperature histories during fabrication and service. As illustrated in Fig. 3 for a typical beam, the temperatures during curing varied with time. The girder was coldest when the concrete was first cast but heated up as the curing process began. Twenty-five hours after casting, the girder cooled when the steam was turned off and the forms were removed.

The temperature histories also varied according to the gage elevation. For example, at the time of maximum temperature gradient, the top temperature (gage TG) was nearly 25°C (45°F) higher than the bottom temperature (gages BL and BR). Such a gradient is consistent with the fabrication conditions. The girders were cast outside when the ambient temperature varied between 0 and 10 °C (32 and 45 °F), so the cold ground cooled the bottom flange. In addition, the steam rose to the top of the insulated blanket covering the girder. The temperature histories also varied slightly from one girder to another, based on the location of the thermocouple that was used to monitor the curing process.

To evaluate the effect of variations of temperature histories on concrete strength, concrete maturities[5] were calculated at the centroid of the prestressing strand for each girder temperature history as follows

$$Maturity = \int \left(T_i(t) + 12.2\right) dt \qquad (1)$$

where $T_i(t)$ = temperature (°C) at location i and time t. As expected, the maturities were lower at the center of gravity of the prestressing strand (gages BL and BR) that at the top of the girder (gage TG). Concrete maturities at the centroid of the prestressing strand, calculated with Eq. 1, are reported in Table 2. Girder 2B had the highest maturity, because

it was subjected to the highest peak temperature. Girder 2A had the next highest maturity, because it was cured for the longest time (Table 1).

During curing, the fabricator's thermocouple was placed at mid-height for all of the girders (except Girder 2B, in which it was placed 457 mm (18 inches) from the bottom of the girder). Consequently, the concrete at the bottom of the girder was weaker than the concrete in the cylinders connected to the Sure-Cure system. Since concrete strength increases with increasing maturity, the concrete in the bottom flange of girders was likely weaker than at other locations. This effect is significant, because at the time the prestressing tendons are released, this location is also the region of highest compressive stress.

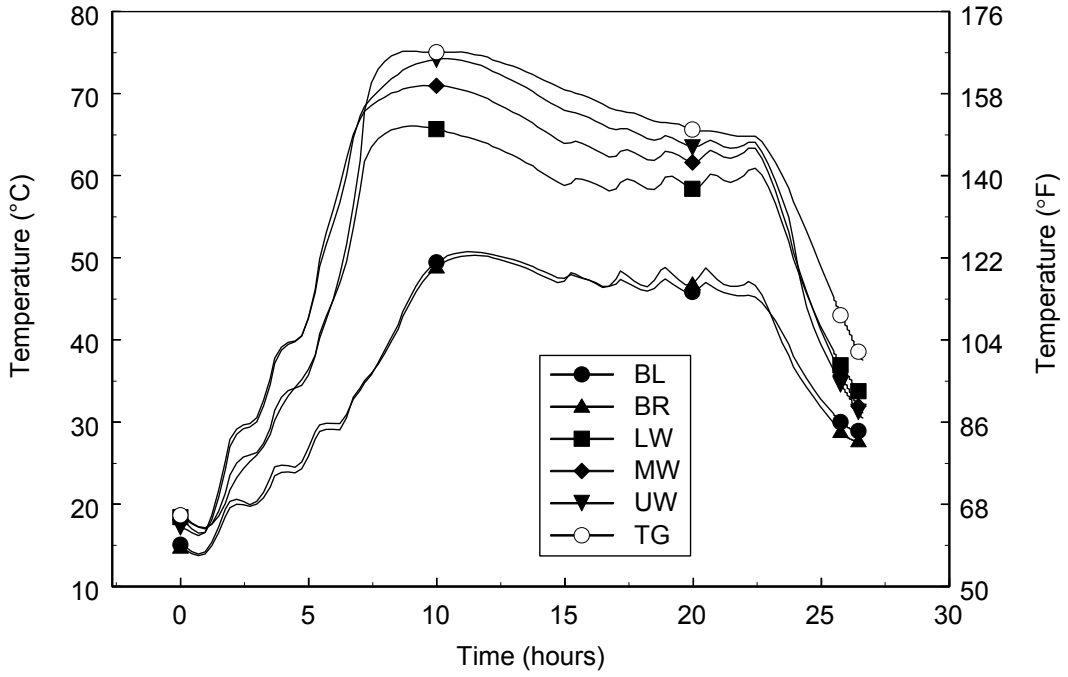

Fig. 3. Typical Temperature Histories During Fabrication

Table 2. Girder Concrete Maturity at cgc at Destressing

Girders	1A	1C	2A	2B	2C
Curing Time at Destressing	24.25	24.25	28.25	25	24
Maturity (˚C-hrs)	1330	1360	1470	1620	1270

OBSERVED CONCRETE STRAINS

The VWSGs also provided nearly continuous readings of longitudinal strain. Strain histories for the midspan of Girder 2B for the first three years of monitoring are shown in Fig. 4.

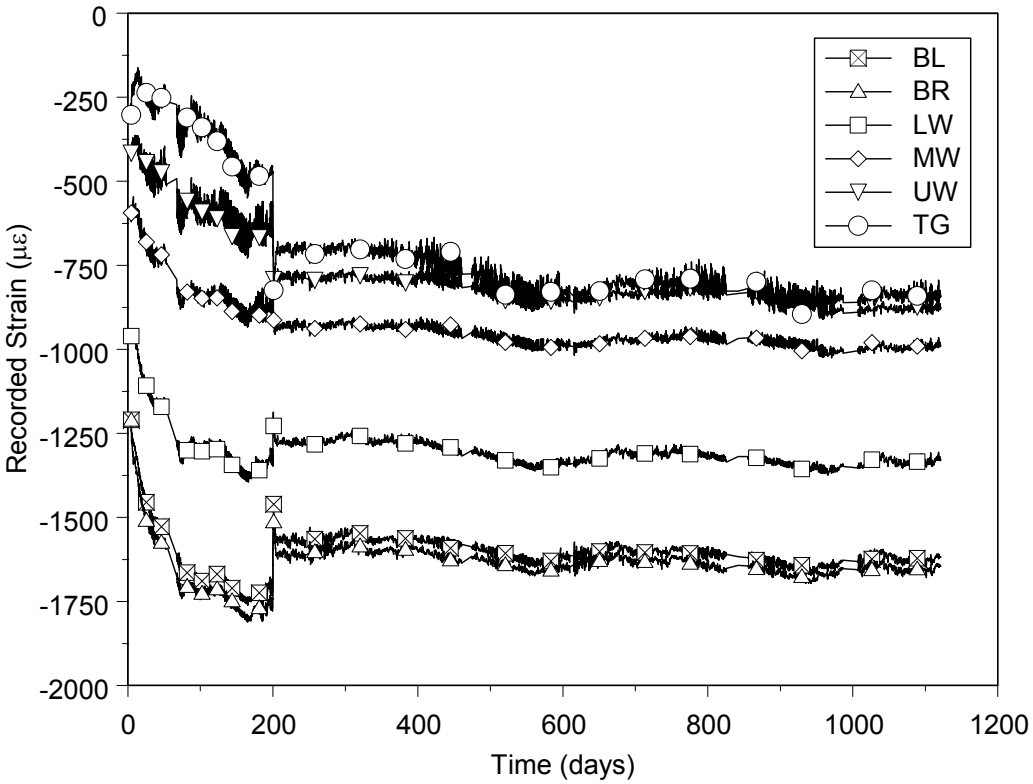

Fig. 4 Service Strains at Midspan of Girder 2B

The abrupt change in strains at day 0 coincides with the release of the prestressing strands. The later changes in measured strains are attributed to creep and shrinkage in the concrete, relaxation of the strand and casting of the bridge deck. The gages towards the bottom of the girder experienced the largest change in strain, as a result of the relatively high stresses. The change in strain measurements for the top gage was smaller, because the stresses were smaller. A small increase in strain occurred after transportation (days 55 to 70). This increase is thought to have been a result of the removal of wooden blocks, which supported the girder in the yard. They provided some frictional resistance at the supports, which in turn led to a positive end moment and reduced camber. Once the girders were lifted off the supports, the girders were free to camber, and the bottom strains increased.

The abrupt change in strain on Day 200 corresponds to casting of the bridge deck. The strains in gages BL, BR and LW decreased while strains increased in gages MW, UW and

TG. As expected, the change in strain was largest in the top (TG) and bottom (BL and BR) gages.

PRESTRESS LOSSES DURING FABRICATION

Prestressing losses were estimated by multiplying the concrete strain measured at the centroid of the prestressing strands (average of gages BL and BR) by the modulus of elasticity of the prestressing steel. Fig. 5 shows a typical strain history at the prestressing centroid during destressing. The strains increased abruptly when the live-end strands were let down. They increased further as the dead-end strands were cut and between the destressing stages. This increase in strain between stages is attributed to creep in the concrete during the destressing operation, which typically lasted about 1 hour. The change in strain due to early creep was estimated as the strain changes that occurred between destressing operations.

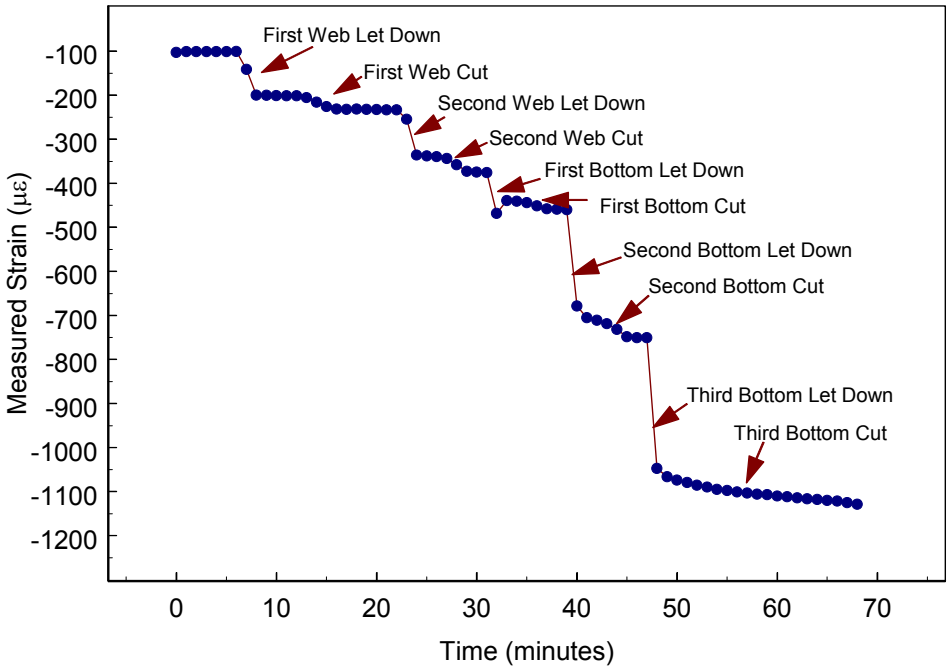

Fig. 5 Strain History at c.g.c. During Destressing at Midspan of Girder 2B

Table 2 lists the stress losses attributable to creep during destressing for the instrumented girders. Girder 2A experienced the largest creep during destressing, which is reasonable, because it also took the longest to destress (2 hours). Girders 2B and 2C had similar stress levels and destressing times, so they experienced similar magnitudes of creep. The early creep losses for girders 1A and 1C were also similar to each other.

Table 3. Early Creep Losses During Destressing

	1A	1B	2A	2B	2C
Change in Strain (με)	49	58	156	106	107
Stress Loss (MPa)	9.7	11.7	30.3	20.7	20.7
Destressing Time (minutes)	72	72	121	68	52

The values for early creep strain were subtracted from the total change in strain during destressing to estimate the strain due to elastic shortening. Table 4 lists the elastic shortening losses computed in this way for each of the instrumented girders. The elastic shortening losses were similar for the two short girders (1A and 1C), corresponding to 5 percent of the jacking stress of 1396 MPa (202.5 ksi). For the long girders, the mean loss corresponds to 14 percent of the jacking stress. As shown in Table 2, the elastic losses were consistent with the expectation that, the lower the maturity value, the larger the elastic shortening, but the effect was small.

Table 4. Elastic Shortening Losses In Instrumented Girders

Girder	1A	1C	2A	2B	2C
Change in Strain (με)	374	353	982	920	985
Stress Loss (Mpa)	73.1	69.6	193	181	194
Maturity (°C-hrs)	1330	1360	1470	1620	1270

PRESTRESS LOSSES DURING SERVICE

After the girders were fabricated, the prestressing force changed due to long-term creep, shrinkage and relaxation, as well as casting of the bridge deck. The effects of creep, shrinkage and deck casting were evaluated from the concrete strains. Prestress loss due to relaxation of the strand in the instrumented girders could not be measured independently from other losses, so a reduced relaxation coefficient[6] was applied to intrinsic relaxation test data obtained from the manufacturer, Sumiden Wire Products Corporation. The change in strain in the prestressing strands due to creep and shrinkage was computed by subtracting the strain due to elastic shortening (Table 4) and deck casting from the average change in strain at the prestressing centroid. Fig. 6 shows the change in strain attributable to creep and shrinkage of the girder concrete and differential shrinkage of the deck at midspan of each instrumented girder.

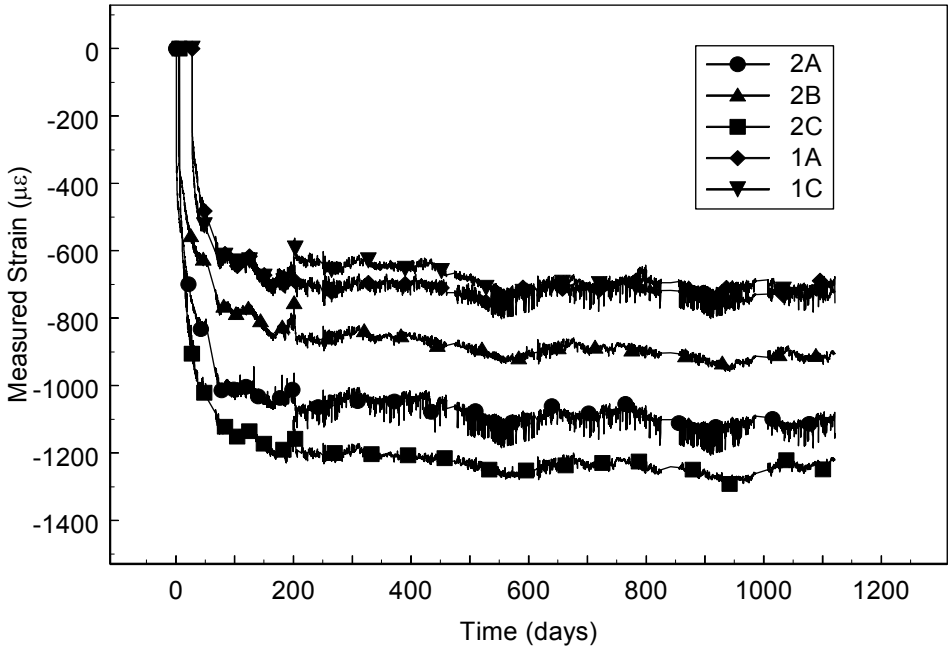

Fig. 6. Change in Strain at Tendon Centroid Due to Creep and Shrinkage

Fig. 6 shows that the two-instrumented girders in Span 1 (1A and 1C) experienced similar changes in strain due to creep and shrinkage. The total strain due to creep and shrinkage at three years is provided in Table 5. The girders in Span 2 experienced different values of creep and shrinkage strain. In particular, Girder 2C experienced the largest change in strain, followed by Girders 2A and 2B.

Tables 5. Losses Due to Creep and Shrinkage (Three Years)

Girders	1A	1C	2A	2B	2C
Change in Strain (με)	688	722	1090	904	1230
Stress Loss (MPa)	135	142	214	178	241
Maturity at Destress (°C-hrs)	1330	1360	1470	1620	1270

Theoretically, the change in strain due to shrinkage of the concrete should be the same for all five girders, because each girder has the same cross-sectional dimensions and concrete mix. Edge girders 1A and 2A might be expected to shrink more, because they were exposed to the sun; however this increase in shrinkage is thought to be small. Therefore the differences between the strain measurements in Fig. 6 are likely due to differences in creep. Since the mix proportions were the same for each girder, the differences between the girders in spans 1 and 2 can be attributed to the different levels of prestress. However, the differences in loss

among the Span 2 girders likely result from differences in maturity at the time of destressing. As was the case with the elastic shortening losses (Table 4), the creep and shrinkage losses in Span 2 were largest for the girder that was the least mature at release (Girder 2C).

The change in stress at midspan due to creep and shrinkage was calculated by multiplying the change in strain (Fig. 6) by the modulus of elasticity of the prestressing strand. Fig. 7 shows the prestress loss due to creep and shrinkage. The same trends that were observed in Fig. 6 are repeated in Fig. 7.

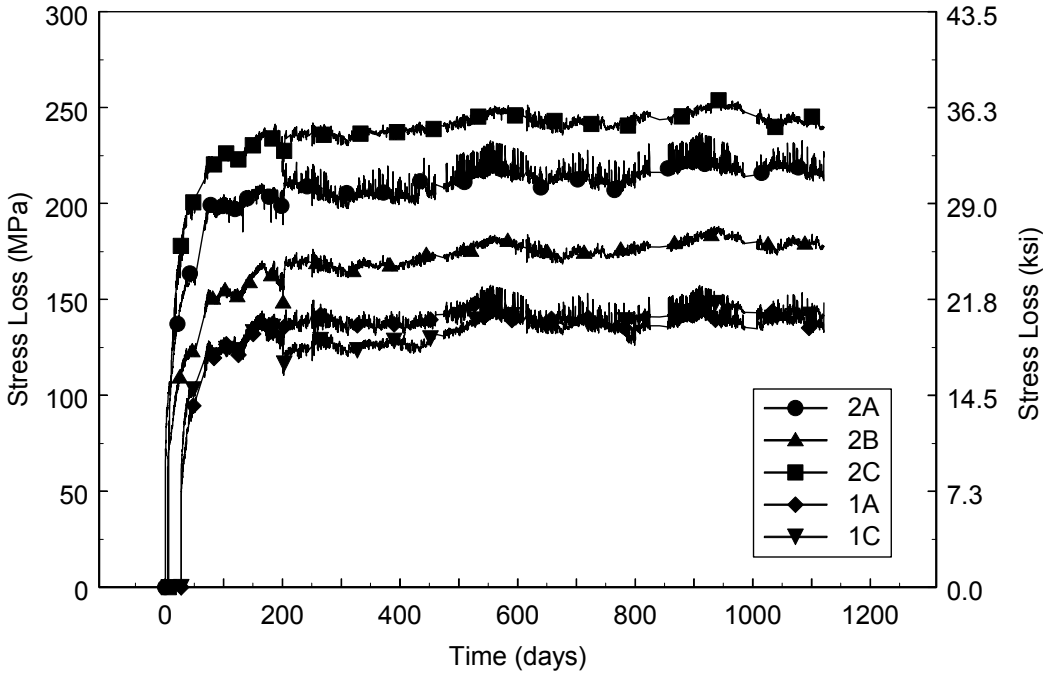

Fig. 7 Prestress Losses Due to Creep and Shrinkage

At day 200, the prestressing strands experienced an abrupt change in strain due to casting of the bridge deck. This change in strain increased the prestressing force. The casting started at 7:30 in the morning and finished at 4:00 in the afternoon. Fig. 8 shows the strain history of Girder 2B from about one week before casting until about one week after casting. The strains in the lower gages (BL, BR and LW) became more tensile, Gage MW had almost no change in strain because it was near the girder neutral axis, and the strains in the upper gages (UW and TG) became more compressive. The heat of hydration from the deck is believed to have caused the top gage (TG) to record higher compressive strains than the upper web gage (UW) for a short period after the casting, but after the hydration finished, the top gage recorded lower compressive strains than any other gage.

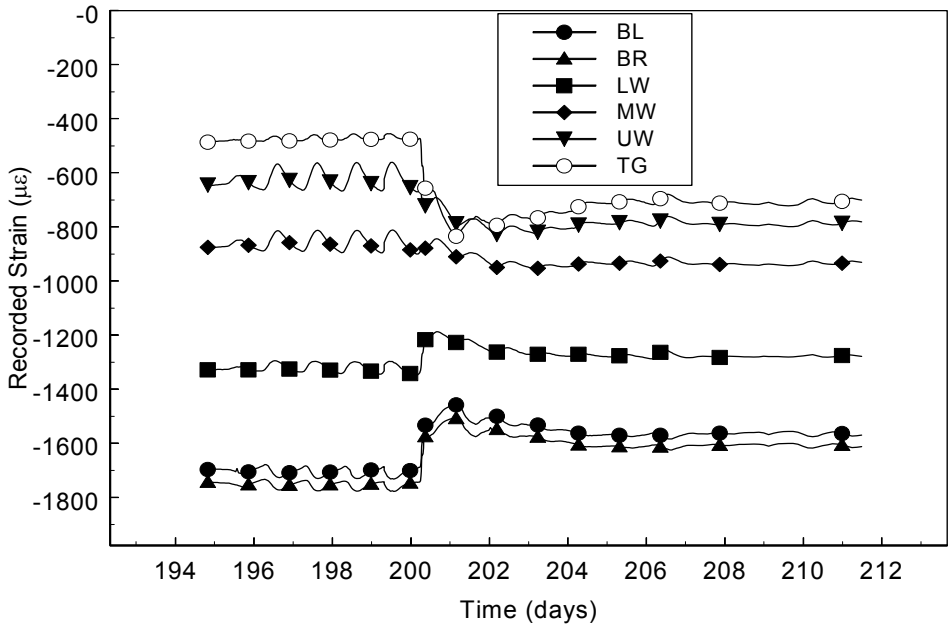

Fig. 8 Girder 2B Deck Casting Strains

The change in stress due to the deck casting was also calculated by multiplying the change in strain by the modulus of elasticity of the prestressing strand. Table 6 lists the measured gain in strand strain at midspan due to the deck casting and the corresponding calculated change in strand stress. Casting of the deck caused a smaller change in stress in the interior girders (1C, 2B and 2C) than in the exterior girders (1A and 2A). This result was surprising, because the tributary slab width for each of the girders is approximately the same. A possible explanation is that the stiff column directly beneath the exterior girders partially restrained their end rotations. The columns did not influence the interior girders as much, so they rotated more freely, thereby incurring more change in strain.

Table 6. Increase in Strand Stress at Midspan Due to Deck Casting

Girder	1A	1C	2A	2B	2C
Measured Change in Strain (με)	77.9	49.5	204	193	175
Change in Strand Stress (Mpa)	15.3	9.72	40.1	37.9	34.4

The change in strain after deck casting, which can be attributed mainly to differential shrinkage, is listed in Table 7. The average change in stress, after the deck casting, was 20.2 and 29.2 MPa (2.9 and 4.2 ksi) for the Span 1 and Span 2 girders. These losses correspond to 1.4 and 2.1 percent of the jacking stress.

Table 7. Losses Due to Creep and Shrinkage After Deck Casting

Girders	1A	1C	2A	2B	2C
Change in Strain (με)	79.1	126	174	146	126
Stress Loss (MPa)	15.5	24.8	34.2	28.7	24.8
% of Total Creep and Shrinkage Strain	11.5	17.5	16.0	16.2	10.2

The reduced relaxation coefficient procedure[6] was applied to the intrinsic relaxation in order to obtain a more accurate estimate of the relaxation losses. The measured values of stress loss due to creep and shrinkage (Fig. 7) were used to obtain the reduced relaxation coefficient for each instrumented girder. The relaxation losses ranged from 1.3 to 1.7 percent of the jacking stress.

EVALUATION OF PRESTRESS LOSS MODELS

The observed values of prestress losses were compared with values calculated using the AASHTO LRFD Specifications[1] and the recommended PCI General Method[2]. All material properties used in these methods were based on their respective design equations, rather than measured values, in order to simulate the estimates that would be made during design.

For the AASHTO Refined Method[1], the total prestress loss at the end of the service life is calculated in a single step. The AASHTO Refined Method was modified into a time-history method in this research by multiplying the ultimate prestress loss predicted by the AASHTO method by the creep and shrinkage coefficients provided in the AASHTO LRFD Specifications. The PCI General Method[2] is a time-stepping algorithm, in which the incremental loss of prestress in each time interval is calculated using the total stress at the start of the interval. The total stress is then updated before calculating the incremental loss in the next interval.

ELASTIC SHORTENING

The measured elastic shortening losses in the instrumented girders (1A,1C, 2A, 2B and 2C), and the elastic shortening losses predicted using the AASHTO LRFD Specifications[1] and the PCI General Method[2] were compared. The assumed value of the modulus of elasticity at transfer (E_{ci}) greatly affects the calculated elastic shortening loss. According to the AASHTO LRFD Specifications[1], E_{ci} should be calculated as

$$E_{ci} = 0.043 w^{1.5} \sqrt{f'_{ci}} \quad \text{(MPa)} \tag{2}$$

where E_{ci} = modulus of elasticity at release of the prestressing strands
= 37.9 GPa (5500 ksi) using Equation 2
w = unit weight of concrete, 2480 kg/m^3 (0.155 kcf) WSDOT design value
f'_c = concrete compressive strength at release (51.0 MPa (7.4 ksi))

However, this equation, which is also used in the ACI Building Code[7], has been found[8] to overestimate the elastic modulus for high-strength concrete, so the ACI 363 Committee Equation, which is specifically for high-strength concrete, was used as a second means to calculate the modulus of elasticity[9].

$$E_{ci} = \left(3320\sqrt{f'_{ci}} + 6900\right)\left(\frac{w}{2320}\right)^{1.5} \quad \text{(MPa)} \tag{3}$$

For the values of w and f'_c listed in Eq. 2, E_{ci} is equal to 33.8 GPa (4900 ksi) using Eq. 3. This value is 11% lower than the value computed with Eq. 2. Fig. 9 compares the predicted elastic shortening losses using the PCI and AASHTO methods with the measured elastic shortening losses for the girders in Span 2. A unit weight of 2480 kg/m^3 (0.155 kcf) was used for all the calculated values. In the figure, the word in the parentheses indicates the source of the equation that was used to calculate the elastic modulus. For example, PCI (AASHTO) means that the value was computed using the PCI method for losses and the AASHTO equation for E_{ci}.

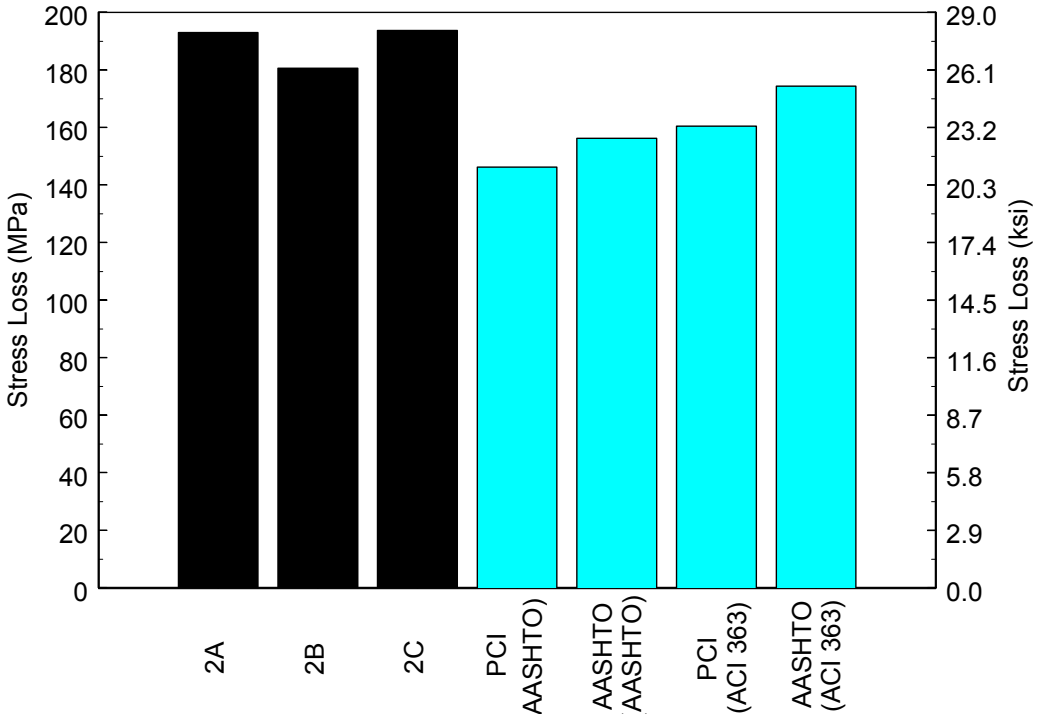

Fig. 9 Observed and Computed Elastic Shortening Losses for Span 2 Girders

The average measured elastic shortening loss for the Span 2 girders was 189 MPa (27.4 ksi). Regardless of the equation used to calculate the initial elastic modulus (Equations 2 or 3), the average measured loss exceeded the predicted loss using either the AASHTO LRFD Method[1] or the PCI Method[2]. The difference between the measured and calculated losses was larger when the elastic modulus was calculated with the equation in the AASHTO LRFD Specifications[1]. This finding would seem to confirm previous research[8] that Eq. 2 overestimates the elastic modulus for high-strength concrete. Even if the modulus of elasticity was calculated using the ACI 363 Equation[9], the elastic shortening losses were still underestimated.

Compared with the PCI exact method, the approximate AASHTO LRFD method predicts elastic shortening losses that were closer to the measured losses. This result does not indicate that the AASHTO method is better than the PCI method. Because the same elastic modulus was used for both methods, the difference lies in the calculation of the initial prestress force. The AASHTO method approximates the initial stress after transfer as $0.7f_{pu}$ (1300 MPa (189 ksi)). This value is higher than the measured initial prestress stress (1396–189 =1207 MPa (202.5-27.4 = 175 ksi)). Essentially, the AASHTO result is closer to the measured losses only because it overestimated the initial prestress.

For the Span 1 girders, the average measured loss was 71.3 MPa (10.3 ksi). The losses were smaller than those in Span 2, because fewer prestressing strands were used. In Span 1, the PCI and AASHTO methods again underestimated the measured elastic shortening losses. As with the Span 2 girders, the predicted elastic shortening losses were closer to the measured losses when the elastic modulus was calculated with the ACI 363 equation (Eq. 3). The elastic shortening losses predicted using the AASHTO LRFD Method and the PCI Method were within 2% of each other, with the PCI Method predicting slightly higher losses. For Span 1, the AASHTO method now predicts lower losses than the PCI method, because the approximated initial prestress (1300 MPa (189 ksi)) is now lower than the actual prestress (1396 - 71.3 = 1325 MPa (202.5 – 10.3 = 192 ksi)).

Two explanations are possible as to why the measured elastic shortening is higher than the predicted: (1) either the calculated elastic modulus was larger than the actual elastic modulus or (2) the estimated values of early creep losses was too low.

Part of the discrepancy between measured and predicted losses can be attributed to using too high a value for the unit weight of concrete. The WSDOT used a value of 2480 kg/m^3 (0.155 kcf) for the unit weight of the concrete. The unit weight of the concrete measured by Central Premix Company was 2400 kg/m^3 (0.150 kcf), which is 3% lower. If the measured unit weight had been used in design, the calculated modulus of elasticity would have decreased by 5%.

Table 8 lists the average observed and predicted elastic shortening losses as a percentage of the total jacking stress for unit weights of 2480 kg/m^3 (0.155 kcf) and 2400 kg/m^3 (0.150 kcf). Table 8 shows that, when the measured value of concrete unit weight (2400 kg/m^3

(0.150 kcf)) was used, the predicted elastic shortening losses were closer to the average measured values.

Table 8. Elastic Shortening Loss as a Percentage of Jacking Stress

	Average Measured	PCI (AASHTO E_c)	AASHTO (AASHTO E_c)	PCI (ACI 363 E_c)	AASHTO (ACI 363 E_c)
w = 2480 kg/m^3					
Span 1	**5.1**	**4.3**	**4.2**	**4.7**	**4.6**
Span 2	**13.5**	**10.5**	**11.2**	**11.5**	**12.5**
w = 2400 kg/m^3					
Span 1	**5.1**	**4.5**	**4.4**	**4.9**	**4.9**
Span 2	**13.5**	**10.9**	**11.8**	**12.0**	**13.1**

Using the PCI exact method for the girders in spans 1 and 2, a modulus of elasticity of 31.0 GPa (4500 ksi) and 28.3 MPa (4100 ksi) respectively would be required to produce the measured observed elastic shortening losses. This value is even smaller than the elastic modulus calculated using the ACI 363 Equation (32.2 MPa (4670 ksi)) with a unit weight of 2400 kg/m^3 (0.150 kcf). Although smaller than the predicted elastic modulus with the ACI 363 equation, the required elastic modulus for spans 1 and 2 falls within the range of measured elastic modulus values from the material samples and could be a result of the lower maturity at the centroid of the prestressing strands at release[10].

The other possible explanation as to why the elastic shortening losses were higher than the predicted losses, was that the procedure for estimating early creep losses during destressing produced values lower than the actual ones. Previously, early creep was defined as any change in strain that occurred between destressing stages. Separating the individual destressing stages from the total destressing time is believed to have been done with reasonable accuracy. However, it is also reasonable to assume that some creep did occur during the destressing stages.

The early creep during the destressing stages was estimated for each of the instrumented girders. For example, for Girder 2B (Fig. 5) the total minutes during destressing (68) were divided into estimated minutes that elastic shortening occurred (17) and estimated minutes during which early creep occurred (51 minutes). The estimated change in stress during the destressing stages could be calculated as the ratio of time attributed to elastic shortening over the total destressing time, multiplied by the estimated change in stress due to early creep losses (Table 3) (i.e. 17/68*20.7 = 5.2 MPa for Girder 2B). For the instrumented girders, the estimated change in stress due to early creep loss during the destressing stages was between 2 to 3% of the measured elastic shortening losses. Because these values are small, it is

believed that the difference between the measured and calculated elastic shortening losses is more likely due to a smaller elastic modulus value than was calculated with equations 2 and 3.

CREEP AND SHRINKAGE

The combination of changes in strain due to creep and shrinkage was measured in the instrumented girders. The calculated prestress losses due to girder shrinkage and creep using the AASHTO LRFD Specifications[1] and the PCI General Method[2] were summed to obtain the combined creep and shrinkage losses. Fig. 10 shows the observed and predicted combined creep and shrinkage losses for the girders in Span 2.

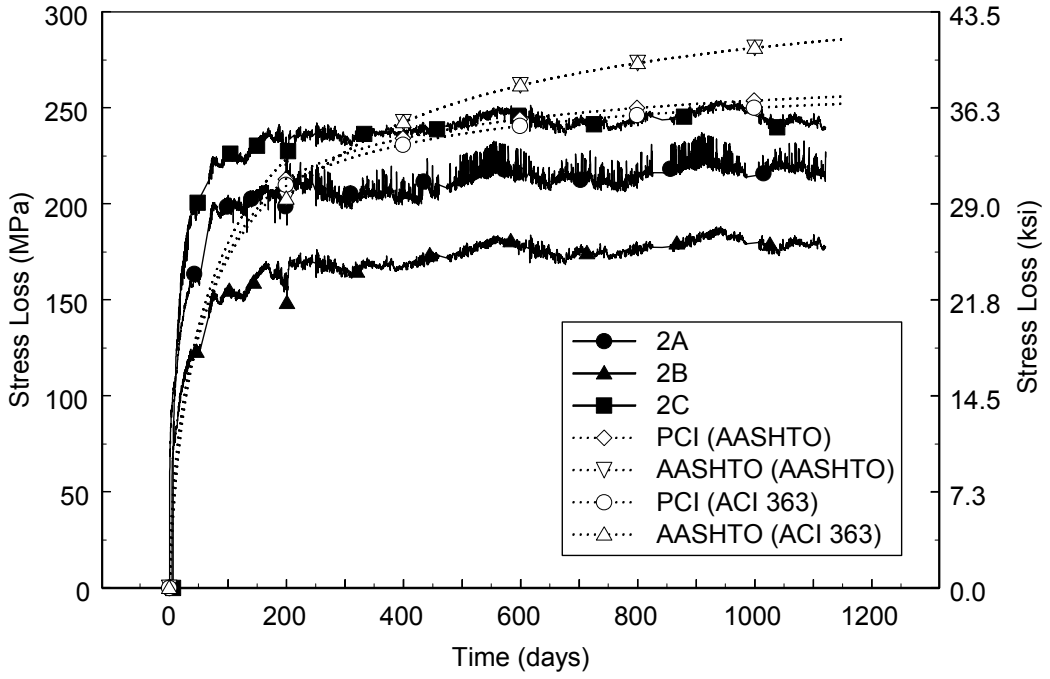

Fig. 10 Observed and Predicted Creep and Shrinkage Losses for Span 2

The creep and shrinkage losses predicted using the AASHTO and PCI methods exceeded the measured creep and shrinkage losses at three years for all three long girders. At three years, the PCI Method was 19% higher than the average measured creep and shrinkage losses, while the AASHTO Method was 34% higher. Both PCI and AASHTO methods produced similar results, regardless of the choice of elastic modulus equation.

For Span 1, the predicted values were lower than the observed values throughout the first three years of the girders' life. The discrepancy was largest initially but therefore diminished with time. The PCI method predicted a creep and shrinkage loss that was closer to the measured values than the AASHTO method. The PCI method predicted shrinkage and creep prestress losses that were about 2% lower than the average measured losses, while the

AASHTO method was 10% lower at three years. Table 9 lists the creep and shrinkage losses for both span girders at three years as a percentage of the initial jacking force.

Table 9. Total Creep and Shrinkage Losses as Percent of the Jacking Stress

Girder	Average Observed	PCI (AASHTO E_c)	AASHTO (AASHTO E_c)	PCI (ACI 363 E_c)	AASHTO (ACI 363 E_c)
Span 1	10.4	10.4	9.4	10.3	9.4
Span 2	15.3	18.8	20.6	18.5	20.6

TOTAL PRESTRESS LOSSES

The total prestress losses due to relaxation of the prestressing strand, elastic shortening, shrinkage, creep and deck casting were added to obtain the total prestress losses. Fig. 11 shows the observed and predicted total prestress losses for the Span 2 girders.

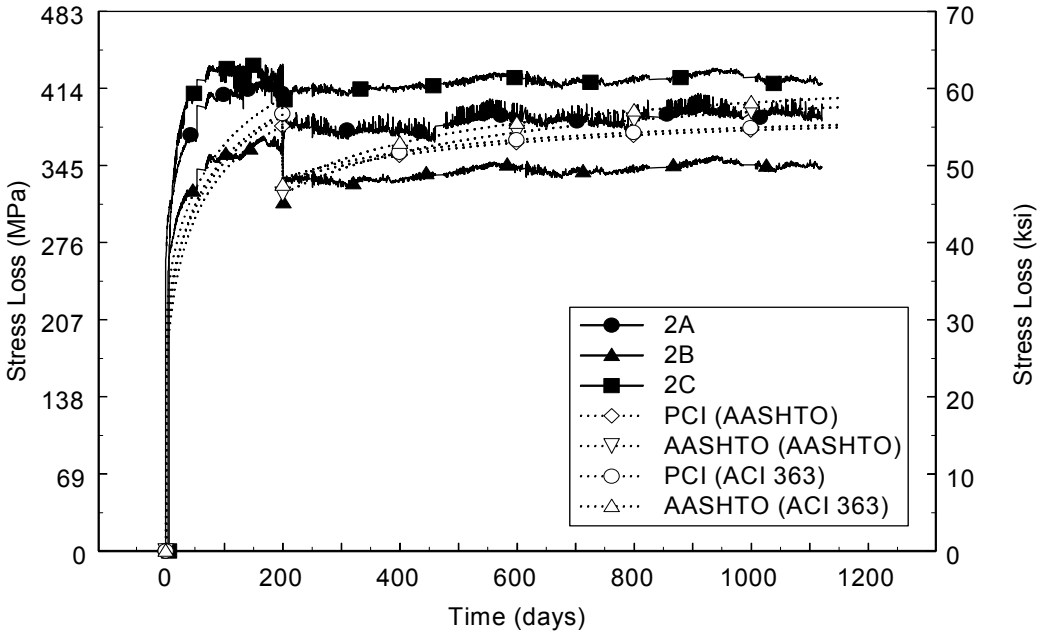

Fig. 11 Total Prestress Losses for Span 2 Girders

Fig. 11 shows that the total observed prestress losses for Span 2 girders are reasonably well predicted by the AASHTO LRFD Specifications[1] and the PCI General Method[2]. The AASHTO method predicts total prestress losses that are slightly higher than the PCI method, mainly because the computed elastic shortening losses are larger. The total losses are slightly larger for the AASHTO method when the ACI 363 elastic modulus equation was

used, but the PCI method predicted nearly identical losses at three years, regardless of which elastic modulus equation was used.

Fig. 12 shows the total observed and predicted prestress losses for the Span 1 girders. The total observed prestress losses for the Span 1 girders are higher than the losses predicted for both the PCI and AASHTO methods. The difference between the observed and predicted values is larger at first and diminishes with time. The PCI method predicts a total prestress loss that is slightly higher than the AASHTO method.

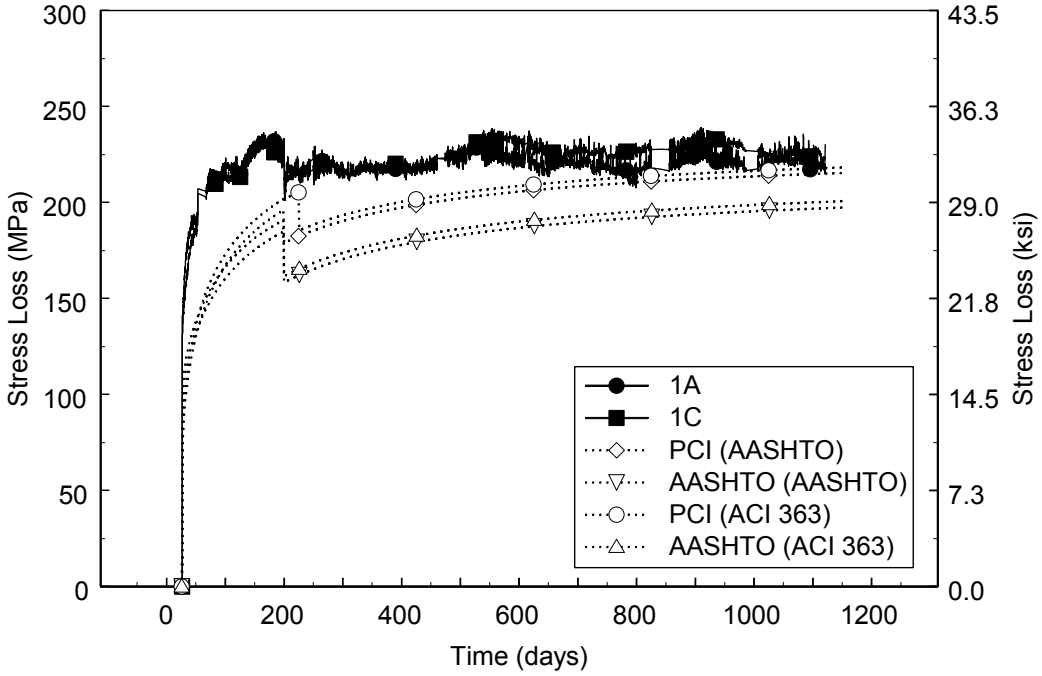

Fig. 12 Total Prestress Losses for Span 1 Girders

The total prestress losses predicted using the AASHTO LRFD Specifications[1] and the PCI General Method[2] were close to the average total measured losses. However, this agreement is not a result of the methods accurately predicting each of the individual components. Instead, the total changes in prestress compared well, because some predictions were too low (e.g., elastic shortening) and others were too high (e.g., creep and shrinkage, relaxation and deck casting). Table 10 lists the total prestress losses at three years as a percentage of the initial jacking stress.

Table 10. Total Prestress Losses at 3 Years as Percentage of Jacking Stress

Girder	Average Observed	PCI (AASHTO E_c)	AASHTO (AASHTO E_c)	PCI (ACI E_c)	AASHTO (ACI E_c)
1A	16.3	15.5	14.2	15.7	14.4
2A	27.6	27.2	28.5	27.3	29.1

CONCLUSIONS

The observed values of prestress losses were compared with values calculated using the AASHTO LRFD Specifications[1] and the recommended PCI General Method[2]. The material properties used in these methods were based on design equations, rather than measured values, in order to simulate the estimates that would be made during design. The study led to the following conclusions:

- During the steam curing, the internal concrete temperatures varied approximately 25 °C (45 °F) over the depth of the girder. The lowest temperatures were recorded at the bottom of the girders, which consequently had the lowest maturity and, by implication, the lowest concrete strength. This curing condition is believed to have influenced the elastic shortening and creep losses.
- The total prestress loss calculated with either the PCI method or the AASHTO Method ranged from 6% lower to 22% higher than the average total observed prestress losses. The calculated total losses were particularly close to the total observed losses when the PCI General Method with an equation specifically for HPC was used to calculate the elastic modulus.
- On average, the observed elastic shortening losses were found to be 8% to 23% higher than the elastic shortening losses calculated with the PCI and AASHTO methods. In comparison to the PCI method, the AASHTO method predicted larger elastic shortening losses for the longer Span 2 girders, but smaller losses for the shorter Span 1 girders.
- The observed losses for creep and shrinkage were between 1% lower to 23% higher than the losses calculated with the PCI method and ranged from 10% lower to 35% higher than the losses calculated with the AASHTO method. The PCI and AASHTO methods over-predicted the creep and shrinkage losses for the Span 2 girders. The AASHTO method under-predicted the creep and shrinkage losses for the Span 1 girder, but the PCI method came fairly close to the observed values.

REFERENCES

1. American Association of State Highway and Transportation Officials (AASHTO). (1998). *LRFD Bridge Design Specifications*, 1st Edition, Washington, D.C.
2. Prestressed Concrete Institute Committee on Prestress Losses (PCI). (1975). "Recommendations for Estimating Prestress Losses." *PCI J.*, 24(4), 44-75.
3. Lwin, M. M. and Khaleghi, B. (1997). "Time-Dependent Prestress Losses in Prestress Concrete Girders Built of High Performance Concrete (Preprint)." Transportation Research Board. 76th Annual Meeting. January.
4. Barr, P., Eberhard, M.O., Stanton, J.F, Khaleghi, B. and Hsieh, J.C. (2000), "High Performance Concrete in Washington State SR 18/ SR 516 Overcrossing: Final Report on Girder Monitoring," Washington State Department of Transportation, Olympia, Washington, December, 150 pp.
5. Lew, H. S. and Richard, T. W. (1978). "*Prediction of Strength of Concrete from Maturity*." ACI Publication SP-56, American Concrete Institute, 229-248.
6. Ghali, A., and Favre, R. (1994). *Concrete Structures Stresses and Deformations.* Second Edition. E & FN Spon. London.
7. American Concrete Institute (ACI) (1995). *Building Code Requirements for Structural Concrete.* Farmington Hills, Michigan.
8. Nawy, E. G. *Fundamentals of High Strength High Performance Concrete.* Longman Group Limited. London. 1996.
9. American Concrete Institute Committee 363 (ACI 363) (1990), Farmington Hills, Michigan.
10. Barr, P., Fekete, E., Stanton, J.F. and Eberhard, M.O. (2000), "High Performance Concrete in Washington State SR 18/ SR 516 Overcrossing: Final Report on Materials Tests," Washington State Department of Transportation, Olympia, Washington, December, 81 pp.